X-ray and electron microscopic determination of Debye characteristic temperature, stacking fault energy and other microstructural parameters in zinc telluride films

U. Pal, S. Saha, B. K. Samantaray, A. K. Chaudhuri and H. D. Banerjee*

Department of Physics and Meteorology, * Materials Science Centre,
Indian Institute of Technology, Kharagpur 721302, India

Zinc telluride | Crystalline films | X-ray diffraction

Abstract. X-ray diffraction, transmission electron microscopy and transmission electron diffraction have been performed on polycrystalline zinc telluride films deposited on glass substrates at different conditions. Along with the cubic phase, the hexagonal phase is detected in the films deposited at 623 K and higher substrate temperatures. Lattice parameters of both phases are calculated from X-ray diffraction and TED data and their variation with the film thickness and substrate temperatures are studied. Cation − cation distances in films of the cubic phase are calculated. Stacking fault energy and Debye characteristic temperature in ZnTe films, their variations with film thickness and substrate temperature are reported for the first time. Attempts have been made to explain the variations in terms of existing theories.

Introduction

Among the II − VI semiconductors, zinc telluride is one of the very important compounds which has the potentiality to be used as γ-ray detectors, solar cells (Parakh, 1987), switching (Patel, 1986) and other opto-electronic devices (Svob et al., 1986; Dean, 1979). The crystalline structure of zinc telluride has been studied by several workers (Zachariasen, 1926; Schubert, 1950; Korneeva, 1960; Cruceanu, 1960; Spînulescu-Carnaru, 1966, 1967;

Ciorăscu et al., 1972; Patel et al., 1983, 1984; Brafman et al., 1964; Brown et al., 1972; Pal et al., 1989). The authors (Zachariasen, 1926; Schubert, 1950; Korneeva, 1960) have studied the crystalline structure of ZnTe powders or monocrystals and concluded that this substance crystallizes in cubic phase only. Cruceanu (1960) has discovered a hexagonal phase along with cubic ones in ZnTe monocrystals grown from gaseous phase. Several workers (Spinulescu-Carnaru, 1966, 1967; Ciorăscu et al., 1972; Patel et al., 1983, 1984; Brafman et al., 1964; Brown et al., 1972; Pal et al., 1989) have studied the crystal structure of ZnTe thin films. They have noticed that the films deposited on glass substrates kept at room temperature have sphalerite structure with one-dimensional stacking disorder. In the films deposited at elevated substrate temperatures, stacking disorder increases and causes the formation of hexagonal crystals of wurtzite type. Kaito et al. (1985) have reported the formation of the hexagonal phase in ZnTe layers on NaCl crystals at elevated temperature (573 K). Brown and Brodie (1972) have also reported the formation of non-crystalline ZnTe thin films on glass substrates kept at low temperatures. However most of those workers dealt with the determination of structure type and a qualitative observation of the defects and grain size from electron microscopy. A quantitative determination of several microstructural parameters like the size of crystallites, microstrain, dislocation density, stacking fault probability has been reported by Pal et al. (1989).

In the present paper, we are reporting for the first time the measured values of r.m.s. displacement of atoms, X-ray Debye temperature and the stacking fault energy of ZnTe films deposited on glass substrates and their dependence on film thickness and substrate temperatures. The lattice constant of the cubic phase is determined from the Nelson-Riley (1945) plots. The cation−cation distance is calculated for the films of different thickness deposited at room temperature and also for the films deposited at different substrate temperatures. Lattice parameters (a, c) for the hexagonal phase which is observed in case of ZnTe films deposited at high substrate temperatures are calculated from their TED patterns.

Experimentals

Films of ZnTe are deposited on properly cleaned glass substrates by evaporating the bulk material from a quartz crucible placed inside a tungsten coil under a vacuum of the order of 10^{-4} Pa with the help of a Hind Hivac Vacuum coating unit (Model 12-A4). The method of synthesis of bulk material has been discussed elsewhere (Pal et al., 1989). The rate of deposition is maintained constant (~ 120 nm min^{-1}). The thickness of the films is measured by a Surfometer (SF 101) as well as by interference method. Films of different thickness are deposited at room temperature (305 K).

Other films are also deposited at different substrate temperatures keeping their thickness almost the same. The deposition of the films at high substrate temperatures is carried out in a suitable apparatus described elsewhere (Santhanam et al., 1982). The composition of the films was measured by EDX analysis using a Camscan Series II DV electron microscope.

The X-ray diffractographs are recorded with the help of a Phillips X-ray diffractometer at a scanning speed of $0.5°/\text{min}$ using $\text{Cu}K_\alpha$ radiation. Transmission electron micrograph and transmission electron diffraction patterns are obtained with the help of an electron microscope (JEOL, JEM 200 CX).

Calculation of crystallite size and microstrain are made with the help of variance analysis of X-ray line profiles. Dislocation densities have been calculated from the particle size and r.m.s. strain values using the relations given by Williamson and Smallman (1956). The stacking fault probabilities are calculated from the peak shift, using the relations given by Warren and Warekois (1955). The detailed analysis of these values have been reported earlier (Pal et al., 1989).

The value of the lattice constant for the cubic phase is determined using Nelson-Riley plots (1945) for the films of different thickness deposited at room temperature and of the order of same thickness deposited at different substrate temperatures. For the determination of the lattice constants of the hexagonal phase the electron diffraction patterns of the hexagonal phase are used. For this purpose the films of ZnTe are deposited on glass substrates at some elevated temperatures (623 K and above). From the hexagonal rings of TED patterns hexagonal lattice parameters are calculated, using the relations

$$a_{ij}^2 = (\lambda^2/3)\frac{A_iB_j - A_jB_i}{B_j\sin^2\theta_i - B_i\sin^2\theta_j} \tag{1}$$

$$c_{ij}^2 = (\lambda^2/4)\frac{A_iB_j - A_jB_i}{A_i\sin^2\theta_j - A_j\sin^2\theta_i} \tag{2}$$

where $A = h^2 + h \cdot k + k^2$, $B = l^2$.

Although the structure of two phases of ZnTe (i.e. cubic and hexagonal) are different, both structures are tetrahedrally co-oriented and in many ways they are similar. Especially (in particular), the local environment of the tetrahedron formed by like atoms in both the structures is identical. Therefore it is meaningful to consider the mean cation — cation distance d_c, for both the phases. For zinc blende structure d_c is related to lattice parameter as $d_c = a/\sqrt{2}$ and for wurtzite, $d_c = a$ and $d_c = \sqrt{3/8}\, c$.

A dislocation may dissociate into two partial ones with an intrinsic fault ribbon in between. In this region the close packed stacking sequence changes

from fcc to hcp in case of fcc alloys and compounds. The stacking fault energy, γ, is the energy per unit area required to produce the fault. If it is low, the fault width will be large and the faults will occur more frequently. Of the different methods used for determining γ, the method of X-ray analysis of the line profiles can be applied to a very wide range of γ values and is readily reproducible. After the publication of Williamson and Smallman's work (1956) many workers have used this X-ray method for the determination of γ. There has been some uncertainty regarding the exact value of constant of proportionality occuring in the relationship between γ, stacking fault probability α and r.m.s. strain. However, from a careful analysis of experimental results, Reed and Schram (1974) have given the exact value of constants of proportionality and the effect of elastic anisotropy has been considered by them. Using this theory (Reed et al., 1974) and considering the fact that a higher degree of accuracy in determining γ can be achieved if the measurement of stacking fault probability α and r.m.s. strain $\langle e^2 \rangle^{1/2}$ are carried out on the same specimen. We have measured the values of γ for zinc telluride films of different thickness at a constant substrate temperature (305 K) and of the order of the same thickness but deposited at different substrate temperatures.

By including the elastic anisotropy term, Reed and Schram (1974) have given the relation

$$\gamma = \frac{K_{111}\,\omega_o\,G_{111}\,a}{\pi\sqrt{3}}\,A^{-0.37}\,\frac{\langle e^2 \rangle_{111}}{\alpha} \tag{3}$$

where $A = 2\,C_{44}/(C_{11} - C_{12})$.

From a careful analysis of experimental data they have obtained the value $K_{111}\,\omega_o$ equals to 6.0. In our calculation of A, we have taken $C_{11} = 7.11$, $C_{12} = 4.07$ and $C_{44} = 3.13 \times 10^{10}$ Nm^{-2} as given by Lee (1970) for ZnTe bulk material.

The values of the integrated intensities for the different X-ray diffraction peaks observed in the diffractograms are corrected for background, thermal diffuse scattering and extinction in the samples following a procedure similar to that described by Mitra and Chattopadhyay (1972). The integrated intensity is given by

$$I = k\,A(\theta)\,L_p\,m|F|^2\,e^{-2B\sin^2\theta/\lambda^2}, \tag{4}$$

where k is the scale factor, $A(\theta)$ the absorption factor, L_p the Lorentz polarization factor, m the multiplicity factor and B is the Debye Waller factor. B is related to the Debye temperature by the relation

$$B = \frac{6\,h^2}{m_a\,KT}\,f(x), \tag{5}$$

where h is Planck's constant, K the Boltzmann constant, T the temperature in K, m_a the mass of the atoms.

$$f(x) = [\Phi(x) x^2 + 1/4x], \Phi(x) = (1/x) \int_0^x \xi \, d\xi / (e^\xi - 1) \text{ and } x = \Theta/T. \quad (6)$$

From equation (4), we have,

$$\ln \frac{I_{obs}}{A(\theta) \, L_p \, m|F|^2} = \text{Constant} - (2 \, B \sin^2\theta)/\lambda^2$$

The plot of $\ln(I_{obs}/I_{cal})$ vs. $(\sin^2\theta)/\lambda^2$ is linear, the slope gives the B value. From the B value $f(x)$ is calculated and from a plot of $f(x)$ vs. x, the value of x and hence the Debye characteristic temperature is calculated.

Results and discussions

The X-ray diffraction patterns of the films of different thickness deposited on glass substrates kept at room temperature (305 K) show that the films
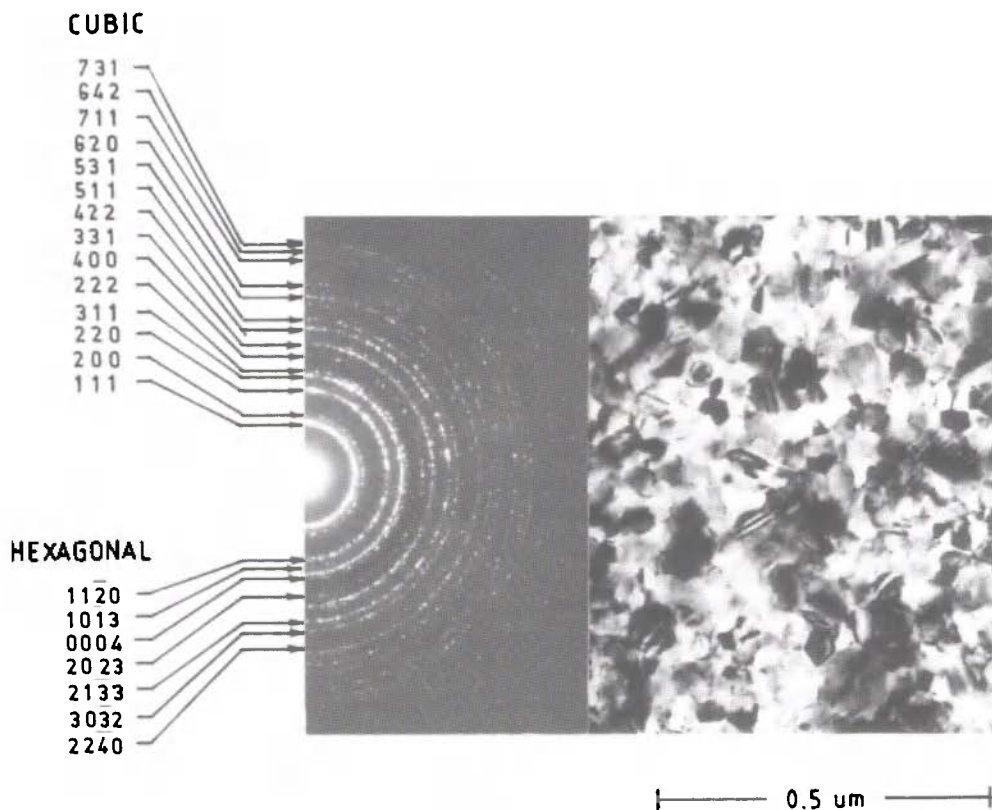

Fig. 1. Transmission electron diffraction (TED) pattern and transmission electron microscopy of ZnTe film deposited at 723 K (57 nm). The cubic and hexagonal rings of TED pattern are indexed separately.
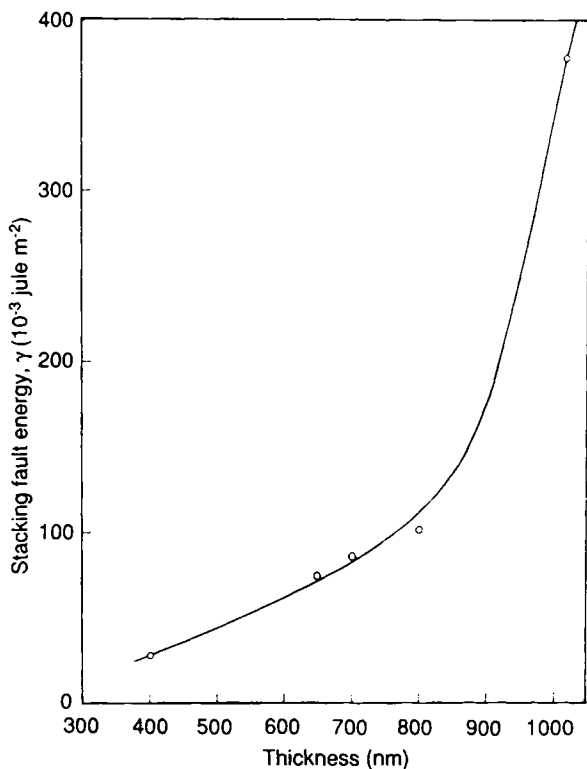
Fig. 2a. Variation of stacking fault energy with the thickness of ZnTe thin films deposited at room temperature (305 K).

are cubic having zinc blende type structure. However a growth of the hexagonal wurtzite type phase is also observed in case of thin films deposited at higher substrate temperatures (623 K and above). This is clearly evident from the TED patterns shown in Figure 1 where the indices of both the cubic and the hexagonal rings are also shown. The lattice parameters of the cubic phases have been calculated from the X-ray diffraction data and that for the hexagonal phases from TED data by the methods discussed earlier. The cation − cation distances for the different films are estimated from the lattice parameter values. The lattice parameter values as well as the cation − cation distances of the films of different thickness are given in Table 1. It is observed that there is a gradual increase in the lattice parameter as well as cation − cation distance with increase in the thickness of the films. It can also be seen from Table 1 that there is a change in the stoichiometry of the films with thickness. The films become Te rich with increase in thicknes. This along with a decrease in the defect content (as evident from
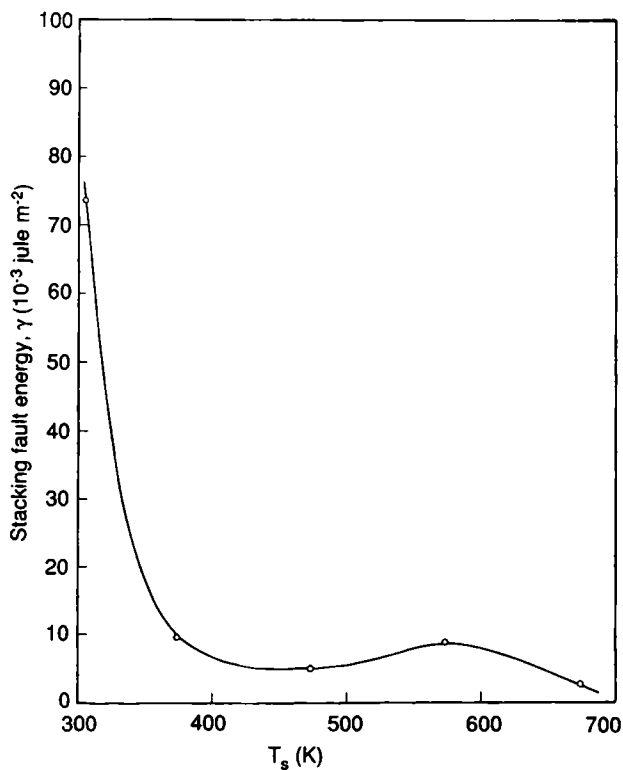
Fig. 2b. Variation of stacking fault energy with substrate temperature of ZnTe thin films (~600 nm).

the decrease in dislocation densities) could be the two main reasons for the gradual changes observed. For the films of nearly same thickness (~600 nm), with increase in substrate temperature, there is a tendency for the lattice parameters to increase and tend towards the bulk values. As reported earlier (Pal et al., 1989) the stoichiometry of the films also improves at higher substrate temperatures. Using the rings corresponding to the hexagonal phase the hexagonal lattice parameters are calculated and the c/a value is observed to be 1.688 and 1.668 for the films deposited at 623 K and 723 K substrate temperatures respectively. Spînulescu-Carnaru (1966) has observed $c/a = 1.645$ for similar films.

The stacking fault probability and r.m.s. strain values for the films as obtained by the method of peak shift and variance analysis have already been reported earlier (Pal et al., 1989). The stacking fault energy values are estimated from the same, following the procedure described earlier. Variation of the stacking fault energy with thickness of the films is shown
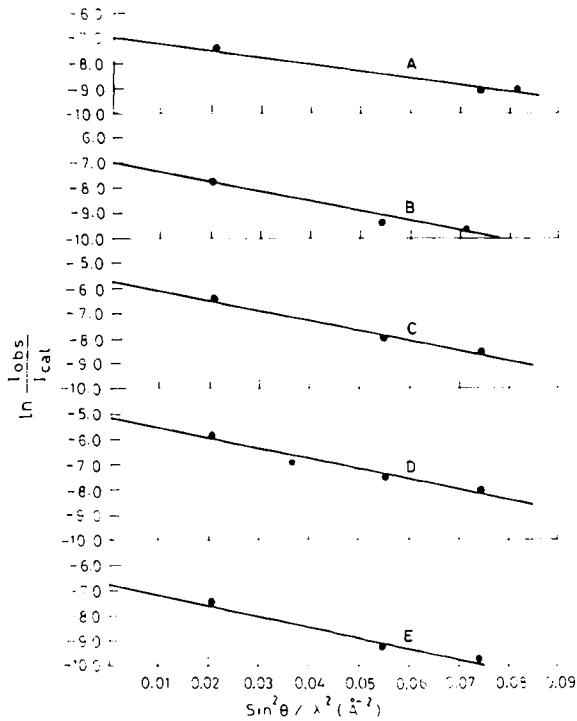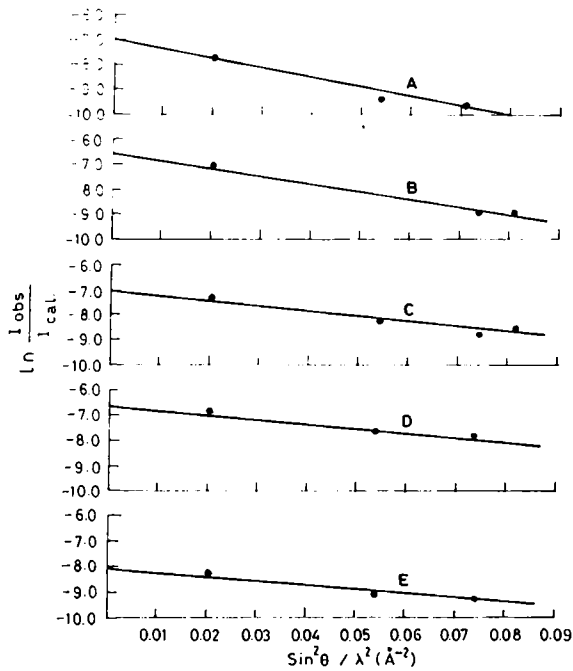
Fig. 3a. Plots of $(\sin^2\theta)/\lambda^2$ Vs. $\ln(I_{obs}/I_{cal})$ for ZnTe films of different thickness (A) 400 nm. (B) 650 nm. (C) 700 nm. (D) 800 nm. (E) 1020 nm deposited at room temperature (305 K).

in Figure 2a and its variation with substrate temperature is shown in Figure 2b. It is observed that with increase in thickness of the films the stacking fault probability falls and the stacking fault energy considerably increases. With increase in substrate temperature the stacking fault energy falls steeply initially and then falls gradually. The value observed in the present case is of the order of 10.0 mJ/m². Rivaud and Desoyer (1983) have reported a value of 13.0 ± 2 mJ/m², Lu and Cockayne (1986) and Takeuchi et al. (1984) have reported the value 16.3 (−1.9 + 2.5) mJ/m² and 16.0 ± 4 mJ/m² in case of thinned ZnTe and bulk ZnTe respectively.

The plots of $\ln(I_{obs}/I_{cal})$ Vs. $(\sin^2\Theta/\lambda^2)$ for ZnTe films of different thickness (T_s = 305 K) and different substrate temperature (∼600 nm) are shown in Figures 3a and 3b. The Debye characteristic temperature values are tabulated in Tables 1 and 2. It is seen that the Debye characteristic temperature decreases gradually with film thickness. The variation of this parameter with film thickness is nominal. Efforts have been made by the

Fig. 3b. Plots of $(\sin^2\theta)/\lambda^2$ Vs. $\ln(I_{obs}/I_{cal})$ for ZnTe films deposited at (A) 305 K (650 nm), (B) 375 K (550 nm), (C) 473 K (600 nm), (D) 573 K (650 nm), (E) 673 K (600 nm).

several workers (Giauque et al., 1937; Rieder et al., 1968; Suzdalev et al., 1967; Roth et al., 1967; Marshall et al., 1966; Petrov et al., 1971; Schoening, 1973) to correlate the variation of Debye characteristic temperature with the thickness and hence the particle size of different films using different techniques of measurements, but the outcomes are inconsistent. From the inelastic neutron scattering studies by radiation damage, Giauque and Achibald (1937) have reported that the heat capacity of small crystallites of MgO is greater than that of large crystals. Inelastic neutron scattering studies by Rieder and Hörl (1968) on MgO crystallites show that the Debye characteristic temperature increases with particle size. Mossbauer effect measurement of the Debye characteristic temperature of small particles of tin (25 nm) by Suzdalev et al. (1967), tungsten (3 nm) by Roth and Hörl (1967) shows that the Debye temperature of the small particles is less than that of bulk whereas in case of gold (6 nm) it has been observed by Marshall and Wilenzick (1966) to be more than bulk value. X-ray

Table 1. Thickness variation of stacking fault energy, X-ray Debye temperature and other microstructural parameters of ZnTe films deposited at room temperature (305 K).

Film thickness	Te/Zn	Lattice constant, a	Dislocation density, ϱ	r.m.s. strain	Stacking fault probability, α	Stacking fault energy	Cation–cation distance, d_c	Debye temperature
(nm)	(at %)	$(10^{-2}$ nm)	$(10^{15}$ lines/m²)	$10^4\langle e^2\rangle^{1/2}$		$(10^{-3}$ J/m²)	$(10^{-2}$ nm)	(K)
400	1.006	60.96	49.5	304	0.351	27.86	43.105	90
650	1.195	61.09	33.8	225	0.073	73.54	43.197	82
700	1.250	61.18	32.8	231	0.067	84.59	43.261	80
800	1.320	61.21	36.9	250	0.067	99.12	43.282	78
1020	1.455	61.23	30.5	291	0.024	375.04	43.296	77

Table 2. Stacking fault energy, Debye temperature and other microstructural parameters of 2nTe films deparited at different substrate temperatures.

Substrate temperature	Film thickness	Te/Zn	Lattice constant, a	Dislocation density, ϱ	r.m.s. strain	Stacking fault probability, α	Stacking fault energy	Cation–cation distance, d_c	Debye temperature
(K)	(nm)	(at %)	$(10^{-2}$ nm)	$(10^{15}$ lines/m²)	$10^4\langle e^2\rangle^{1/2}$		$(10^{-3}$ J/m²)	$(10^{-2}$ nm)	(K)
305	650	1.195	61.09	33.8	225	0.073	73.54	43.197	81
373	550	1.120	60.97	13.0	99	0.109	9.52	43.112	92
473	600	1.100	60.99	7.9	61	0.079	4.99	43.126	96
573	650	1.060	61.11	7.1	105	0.085	13.75	43.211	97
673	600	1.095	61.04	19.4	80	0.266	2.55	43.162	98

measurements for copper and gold by Petrov and Kotel'nikov (1971) shows a reduction in Debye temperature for small particles. Using LEED, Schoening (1973) has observed a 20% decrease in the Debye temperature of gold crystallites with a decrease in crystallite size from 29.4 nm to 3.5 nm.

In the case of our ZnTe films of different thickness particle size slowly increases with the film thickness and sharply with the increase of substrate temperature (Pal et al., 1989). The stoichiometry deviates more with the increase of film thickness and a betterment with the increase of substrate temperature. Though the particle size increases (slowly) with the increase of film thickness but the sharp deviation of stoichiometry can be attributed to the reason for slow decrease of Debye characteristic temperature. The result is a cumulative effect of both the factors. For the films deposited at different substrate temperatures, though the composition approaches slowly towards its stoichiometry but the particle size increases sharply and hence Debye characteristic temperature. The Debye characteristic temperature of ZnTe has been calculated from the specific heat measurements by Aggarwal and Verma (1972) and Lee (1970) and is found to be 225.2 ± 0.1 K at absolute zero. We have calculated the Debye characteristic temperature for polycrystalline ZnTe powder at room temperature (305 K) from X-ray diffraction data and obtained the value 196 K, which is far greater than the values obtained for thin films.

Conclusions

Particle size of ZnTe films increases with its thickness and with the substrate temperature. Hexagonal phase appears along with the cubic one at 623 K and above substrate temperatures. The lattice parameter for cubic phase approaches towards the bulk value as the composition of the films approaches towards stoichiometry. The c/a for hexagonal phase equals to 1.688 and 1.668 for the films deposited at 623 K and 723 K respectively which are slightly greater than reported values (Spinulescu-Carnaru, 1966). The stacking fault energy for the films of different thickness increases with their thickness. Stacking fault energy decreases with the increase of substrate temperature and becomes almost constant at higher temperatures. The value of stacking fault energy for stoichiometric films ($T_s = 623$ K and above) is of the order of 10.0 mJ/m^2 whereas the reported values of it for bulk ZnTe are 13.0 ± 2 mJ/m^2 (Rivaud et al. 1983), $16.3\,(-1.9 + 2.5)$ mJ/m^2 (Lu et al., 1986) and 16.0 ± 4 mJ/m^2 (Takeuchi et al., 1984) respectively. The value of cation–cation distance increases with the increase of thickness of the films and hence the r.m.s. displacement of the atoms causing the decrease of Debye characteristic temperature. The sharp increase of particle size with substrate temperature (Pal et al., 1989) increases the value of Debye temperature.

References

Aggarwal, M. D., Verma, J. K. D.: Debye temperatures of cubic $A^{III}B^V$ and $A^{II}B^{VI}$ Semiconductors. Indian J. Pure Appl. Phys. **10** (1972) 838 – 839.

Brafman, O., Alexander, E., Fraenkel, B. S., Kalman, Z. H., Steinberger, I. T.: Polar properties of ZnS crystals and the anomalus photovoltatic effect. J. Appl. Phys. **35** (1964) 1855 – 1860.

Brown, H. M., Brodie, D. E.: Structure and electrical conductivity of amorphous ZnTe and CdTe. Can. J. Phys. **50** (1972) 2512 – 2519.

Ciorăscu, F., Spinulescu-Carnaru, I., Stanescu, C.: The dependence of the electrophysical properties of ZnTe thin films on stoichiometry. Phys. Status Solidi (a) **9** (1972) 449 – 454.

Cruceanu, E.: Thesis, Moscow (1960)

Dean, P. J.: Opto electronic studies on refined ZnTe and implications for II – VI semiconductors. J. Lumin. **18 – 19** (1979) 755 – 756

Giauque, W. F., Archibald, R. C.: Entropy of water from third law of thermodynamics. J. Am. Chem. Soc. **59** (1937) 561 – 569.

Kaito, C., Nakamura, N., Saito, Y.: High resolution electron microscopic studies of the oxidation process of ZnTe films. Appl. Surf. Sci. **22 – 23** (1985) 604 – 612.

Korneeva, I. V.: Thesis, Moscow (1960)

Lee, B. H.: Elastic constants of ZnTe and ZnSe between 77 K – 300 K. J. Appl. Phys. **41** (1970) 2984 – 2987.

Lu, G., Cockayne, D. J. H.: Partial separation of extended x and β dislocations in II – VI semiconductors. Philos. Mag. (A) **53** (1986) 307 – 320

Marshall, S. W., Wilenzick, R. M.: Effect of crystal size on Mössbauer recoil-free fraction in Au^{197}. Phys. Rev. Lett. **16** (1966) 219 – 221.

Mitra, G. B., Chattopadhyay, T.: Effect of defects on the Debye characteristic temperatures of nickel and copper-nickel alloys. Phys. Status Solidi (a) **9** (1972) 89 – 96.

Nelson, J. B., Riley, D. P.: An experimental investigation of extrapolation methods in the derivation of accurate unit-cell dimensions of crystals. Proc. Phys. Soc., London **57** (1945) 160 – 177.

Pal, U., Saha, S., Samantaray, B. K., Banerjee, H. D., Chaudhuri, A. K.: X-ray line broadening and electron microscopic studies on ZnTe thin films. Phys. Status Solidi (a) **111** (1989) 515 – 522.

Pal, U., Saha, S., Chaudhuri, A. K., Rao, V. V., Banerjee, H. D.: Some optical properties of evaporated zinc telluride films. J. Phys. D.: Appl. Phys. **22** (1989) 965 – 970.

Patel, N. G.: Some observations on the switching and memory phenomena in ZnTe-Si. J. Mater. Sci. **21** (1986) 2097 – 2099.

Patel, S. M., Patel, N. G.: Optimization of growth conditions for ZnTe films. Mater Latter. **2** (1983) 131 – 133

Patel, S. M., Patel, N. G.: Switching mechanism in ZnTe films. Thin Solid Films. **113** (1984) 185 – 188.

Parakh, N. C.: Conduction mechanism in zinc telluride films. Indian J. Pure Appl. Phys. **25** (1987) 110 – 113.

Petrov, Yu. I., Kotel'nikov, V. A.: Debye-Waller factor and lattice parameter of small metal particles. Sov. Phys.-Solid State **13** (1971) 255 – 257.

Reed, R. P., Schram, R. E.: Relationship between stacking fault energy and X-ray measurement of stacking fault probability and microstrain. J. Appl. Phys. **45** (1974) 4705 – 4711.

Rieder, K. H., Hörl, E. M.: Search for surface modes of lattice vibrations in magnesium oxide. Phys. Rev. Lett. **20** (1968) 209 – 211.

Rivaud, G., Desoyer, J. C.: Plastic deformation of II – VI compounds with sphalerite structure, example ZnSe, ZnTe. J. Phys. (Paris) **44** (1983) C4 – 387.

Roth, S., Hörl, E. M.: Decrease of Mössbauer recoil-free fraction in small tungsten particles. Phys. Lett. **25A** (1967) 299 – 300.

Santhanam, S., Samantaray, B. K., Chaudhuri, A. K.: Effect of substrate temperature on SnTe films. J. Phys. D.: Appl. Phys. **15** (1982) 2531 – 2535.

Schoening, F. R. L.: Influence of crystal size on electron diffraction intensities. J. Appl. Crystallogr. **6** (1973) 145 – 148.

Schubert, K.: On the discussion of crystal structures. Z. Naturforsch. **5a** (1950) 345 – 346.

Spinulescu-Carnaru, I.: The crystalline structure of ZnTe thin films. Phys. Status Solidi **18** (1966) 769 – 778.

Spinulescu-Carnaru, I.: The orientation of crystallites in ZnTe thin films. Phys. Status Solidi **23** (1967) 157 – 163.

Suzdalev, I. P., Gen, M. Ya., Gol'danskii, Makarov, E. F.: Nuclear Gamma resonance in highly dispersed tin. Sov. Phys. JETP. **24** (1967) 79 – 80.

Svob, L., Marfaing, Y.: Hydrogen-acceptor interaction in CdTe and ZnTe studied by photoluminescence. Solid State Commun. **58** (1986) 343 – 346.

Takeuchi, S., Suzuki, K., Maeda, K., Iwanaga, H.: Stacking-fault energy of II – VI compounds. Philos. Mag. (A) **50** (1984) 171 – 178.

Warren, B. E., Warekois, E. P.: Stacking faults in cold-worked alpha-brass. Acta Metal **3** (1955) 473 – 479.

Williamson, G. K., Smallman, R. E.: Dislocation densities in some annealed and cold worked metals from measurements on the X-ray Debye Scherrer Spectrum. Philos. Mag. **1** (1956) 34 – 46.

Zachariasen, W.: Über die Kristallstruktur der Telluride von Beryllium, Zink, Cadmium und Quecksilber. Z. Phys. Chem. **124** (1926) 277 – 284.